



H2020-ICT-25-2016-2017



**HYbrid FLying rollIng with-snakeE-aRm robot for contact inSpection**

## **HYFLIERS**

### **D5.1**

#### *Hybrid robot hardware integration*

<b>Contractual date of delivery</b>	31 May 2022
<b>Actual date of delivery</b>	7 Oct 2022
<b>Editor(s)</b>	P. J. Sanchez-Cuevas (CATEC)
<b>Author(s)</b>	P.J. Sanchez-Cuevas (CATEC), D. Neva (USE), R. Schmid (WTR), V. Lippiello (CREATE), Miguel A. Trujillo (CATEC), G. Heredia (USE), A. Viguria (CATEC) and A. Ollero (USE), Ulrico Celentano (UOULU), Marko Kauppinen (UOULU), Juha Röning (UOULU), Miika Sikala (UOULU)
<b>Workpackage</b>	WP5
<b>Estimated person-months</b>	42
<b>Dissemination level</b>	PU
<b>Type</b>	DEM
<b>Version</b>	1.0
<b>Total number of pages</b>	33

#### **Abstract:**

This document is about the final integrated version of the versatile hybrid robots for contact inspection with application to pipe inspection. Two prototypes are presented to accomplish the inspection applications. The document includes a high-level system architecture and specifies the final version of the aerial platform, as well as a description of the inspection devices and a short description of the UT sensor integration.

#### **Keywords:**

Hybrid robot. Aerial robot. Satellite robot. Magnetic attractor. Hyper-redundant robotic arm. UT inspection. Miniature UT probe. Pipe inspection. Remote inspection. Refinery. Operations support. Ground station. Emergency behaviour. Ground support. Battery management. Inspection data management.

## **Executive summary**

This document describes the integrated version of the hybrid robot prototypes developed in the HYFLIERS project from the hardware point of view. Based on the initial system specification (D1.1) and following the consideration of the system concept architecture (D1.2) and following the work of previous design deliverables (D2.1 and D2.2) two different prototypes were proposed in the HYFLIERS use case. Each one has different scope and is targeting different technology readiness level (TRL). According to the proposal, the Hybrid Mobile Robot (HMR) aims to be positioned with a Technology Readiness Level (TRL) 6, however, some parts of the HMR system will reach higher TRLs. This will be the case of the inspection satellite mounted in the flying platform. In contract, the Hybrid Robot with Arm (HRA) aims to push the state-of-the-art a little bit more through innovative and original concepts. As a consequence, HRA developments target a TRL 5.

This document clarifies the final integrated version of both prototypes in the shape of a prototype deliverable and describes all the subsystems included in their final form.

The results collected in this deliverable (D5.1) in combination with the D5.2 and D5.3, show that both robot and their different subsystems were successfully tested through several experiments in controlled scenarios, and they are ready to start the validation phase along with the WP6.

## Abbreviations and symbols

BMS	Battery Management System
CAN	Controller Area Network
CATEC	Centro Avanzado de Tecnología Aeroespaciales
CMD	Command prompt
CoM	Centre of Mass
CREATE	Consorzio C.R.E.A.T.E.
DB	Database
DBUS	Desktop Bus
DC	Direct Current
DN	Diameter Nominal
DoF	Degree of Freedom
EC	European Commission
ETH	Ethernet
ESC	Electronic Speed Controller
FPV	First Person View
FRR	Full Requirement Robot
FuMo	Functional Model
GS	Ground Station
GPS	Global Positioning System
HD	High Definition
HDMI	High Definition Multimedia Interface
HLC	High Level Computer
HYFLIERS	Hybrid flying rolling with-snake-arm robot for contact inspection
HMR	Hybrid Mobile Robot
HR	Hybrid Robot
HRA	Hybrid Robot w/ Arm
ICT	Information and communications technology
IMU	Inertial Measurement Unit
GCS	Ground Control Station
LCD	Liquid Crystal Display
LiPo	Lithium-Polymer
LRR	Limited Requirement Robot
MSP	Mobile Support Platform
MTOW	Maximum Take-Off Weight
ORB	Oriented fast and Rotated BRIEF
PC	Personal Computer
PPM	Pulse-Position Modulation
PWM	Pulse Width Modulation
RGB	Red Green Blue
ROS	Robot Operating System

RPA	Remotely Piloted Aircraft
SAP	Snake Arm with pan and tilt Probe
SLAM	Simultaneous Localization And Mapping
TRL	Technology Readiness Level
TX	Transmitter
UAV	Unmanned Aerial Vehicle
UI	User Interface
UOULU	University of Oulu
USB	Universal Serial Bus
USE	Universidad de Sevilla
UT	Ultrasonic
VMC	Visual Meteorological Conditions
VSLAM	Visual Simultaneous Localization and Mapping
WP	Workpackage
WTR	Waygate Technologies Robotics

## Table of Contents

Executive summary .....	2
Abbreviations and symbols .....	3
1. Final hybrid robot hardware integration .....	8
2. HMR final prototype .....	9
2.1. Aerial System .....	10
2.2. Final integrated localisation and obstacle avoidance system .....	11
2.3. Ultrasonic System .....	12
2.4. Integrated satellite robot .....	15
2.5. Magnetic Landing Gear for non-insulated pipes .....	17
2.6. Umbilical Mechanism .....	18
2.7. General connections and communications .....	19
3. HRA final prototype .....	20
3.1. HRA final aerial platform .....	21
3.2. Final landing gear for single pipes .....	22
3.3. Integrated HRA C-tool manipulator and ultrasonic sensor .....	23
3.4. Integrated HRA final prototype .....	27
4. Ground segment systems .....	29
4.1. MSP cart System .....	29
4.2. MSP Support Computer .....	30
4.3. Inspection Data Management .....	31
5. Conclusions .....	32
References .....	33

## List of figures

Figure 1 HMR overview. ....	9
Figure 2 HMR system architecture. ....	10
Figure 3. Final prototype of the HMR robot. ....	10
Figure 4 Final cameras position. ....	11
Figure 5 Final mounting system of the tracking cameras shown in detail. ....	11
Figure 6 Final position of the depth cameras shown in detail. ....	12
Figure 7 UT unit installed on the drone. ....	12
Figure 8 Channel configuration. ....	13
Figure 9 PULLUP resistor encoder. ....	14
Figure 10 Encoder cable short circuit prevention. ....	14
Figure 11 Circuits to prevent the polarity inversion (left) and to extend power supply range (right). ....	15
Figure 12 HMR satellite. ....	15
Figure 13 Satellite camera and feed. ....	16
Figure 14 Inspection sensor and couplant management. ....	16
Figure 15 Performing a longitudinal line scan on a straight pipe section. ....	17
Figure 16 Final landing gear. ....	17
Figure 17 Landing gear magnets design and “as built” shown in detail. ....	17
Figure 18 Landing gear magnets shown in detail. ....	18
Figure 19 Cable rolling final system. ....	18
Figure 20 Slipping used for the cable rolling movement. ....	19
Figure 21 Ubiquiti AC mounted in the drone and network architecture. ....	19
Figure 22 Main hardware subsystems of the HRA. ....	20
Figure 23 Systems hierarchy of the HRA. ....	20
Figure 24 HRA final aerial platform overview (without propellers). ....	21
Figure 25 Autopilot and onboard computer wiring scheme. ....	22
Figure 26 Final landing gear for single pipes. ....	22
Figure 27 Wheel systems for the final landing gear. ....	23
Figure 28 Active (left) and passive (right) wheels for the final landing gear. ....	23
Figure 29 Kinematic frame of the C-Tool. A5 represents the rotation frame of the tool. ....	24
Figure 30 (Left) C-Tool electronics (Right) C-Tool water pump. ....	24
Figure 31 C-Tool over the pipe. ....	25
Figure 32 C-Tool: front view. ....	25
Figure 33 Detaching mechanism to perform the thickness measurement. ....	26
Figure 34 C-Tool: internal components. ....	26
Figure 35 Tool with EMAT sensors: detail of the EMAT detaching mechanism. ....	27
Figure 36 Complete integration of the multirotor platform and the C-Tool. ....	28
Figure 37 Complete video sequence of a mission performed by the platform. ....	28
Figure 38. HYFLIERS global architecture. ....	29
Figure 39. Implemented MSP main battery system used in functional testing. ....	30
Figure 40. Left: MSP Support computer box. Right: Custom battery charging and power-path control board. ....	30

**List of tables**

Table 1 Main Characteristic UT unit table..... 13

Table 2 New BandWidth of the UT unit: a) Low frequency, b) High frequency ..... 14

# 1. Final hybrid robot hardware integration

This deliverable outlines the final hardware integration of the hybrid robots developed in the HYFLIERS project. It is important to remark that according to both the previous deliverables and the project proposal, the consortium has developed two different robotic systems in the context HYFLIERS project. Those systems are targeting different inspection scenarios and have been developed with different TRL.

The two approaches can be summarized as follows:

- **Hybrid Mobile Robot (HMR):** This robot is focused on magnetic pipe inspection. It is a hybrid robot that can take-off, fly, land and move on a pipe to perform the inspection required by the end-users. This system is focused on the magnetic pipes inspection, and it is composed of an aerial vehicle adapted to the industrial environment and a satellite vehicle with the capability of crawling along the pipe to carry out the pipe inspection with the sensors mounted on-board.
- **Hybrid Robot with Arm (HRA):** The HRA is focused on magnetic and non-magnetic pipe inspection using a lightweight robotic arm with an ultrasonic (UT) probe. The system will be able to land on magnetic and non-magnetic isolated pipes and pipe racks. It consists of a modular aerial platform and different add-ons which will be used depending on the application. Due to HRA is targeting a wider range of application and more challenging scenarios (magnetic and non-magnetic pipes and pipe racks), this prototype is expected to have a lower TRL. Instead, it is expected to generate a greater scientific impact driven by a more significant innovation.

According to the proposal, the Hybrid Mobile Robot (HMR) aims to be positioned with a TRL 6, however, some parts of the HMR system will reach higher TRLs. This will be the case of the inspection satellite mounted in the flying platform. In contrast, the Hybrid Robot with Arm (HRA) aims to push the state-of-the-art a little bit more through innovative and original concepts. As a consequence, HRA developments target a TRL 5.

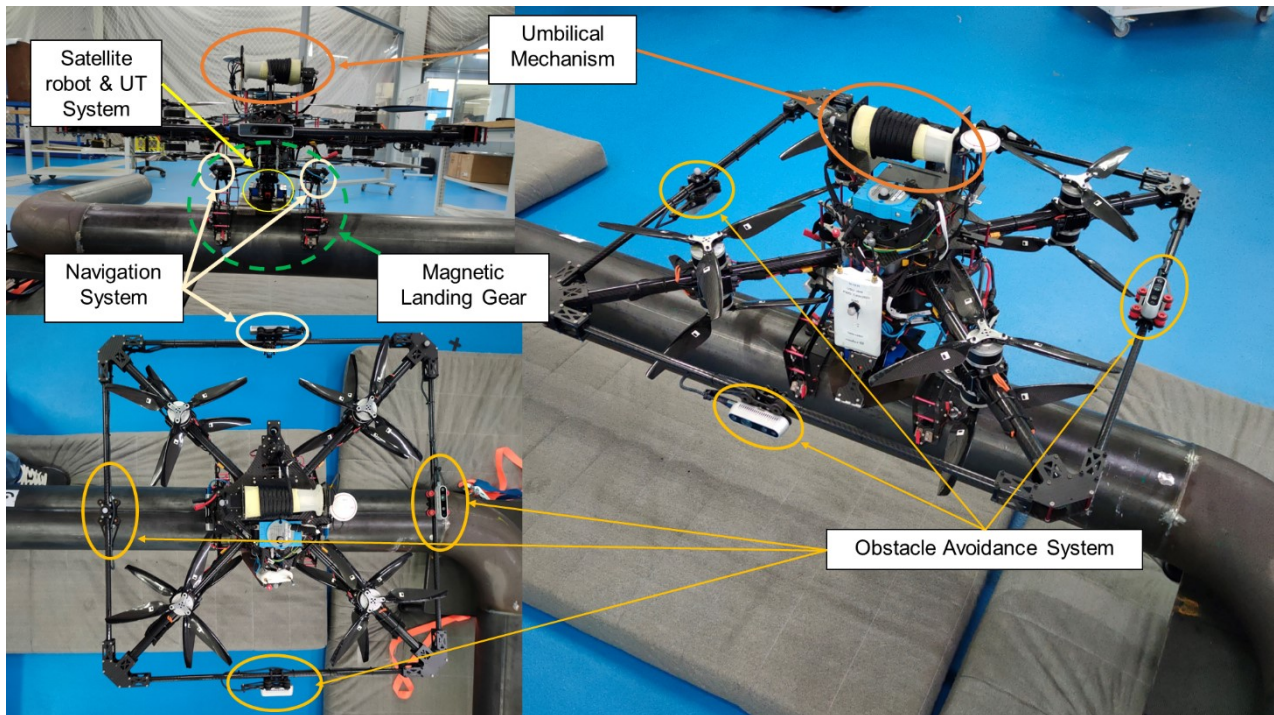
As it was mentioned above, the rest of the document described in detail the different hardware components that integrates both prototypes. The authors of this deliverable strongly recommend the readers to follow this document and the D5.2 together.



## 2. HMR final prototype

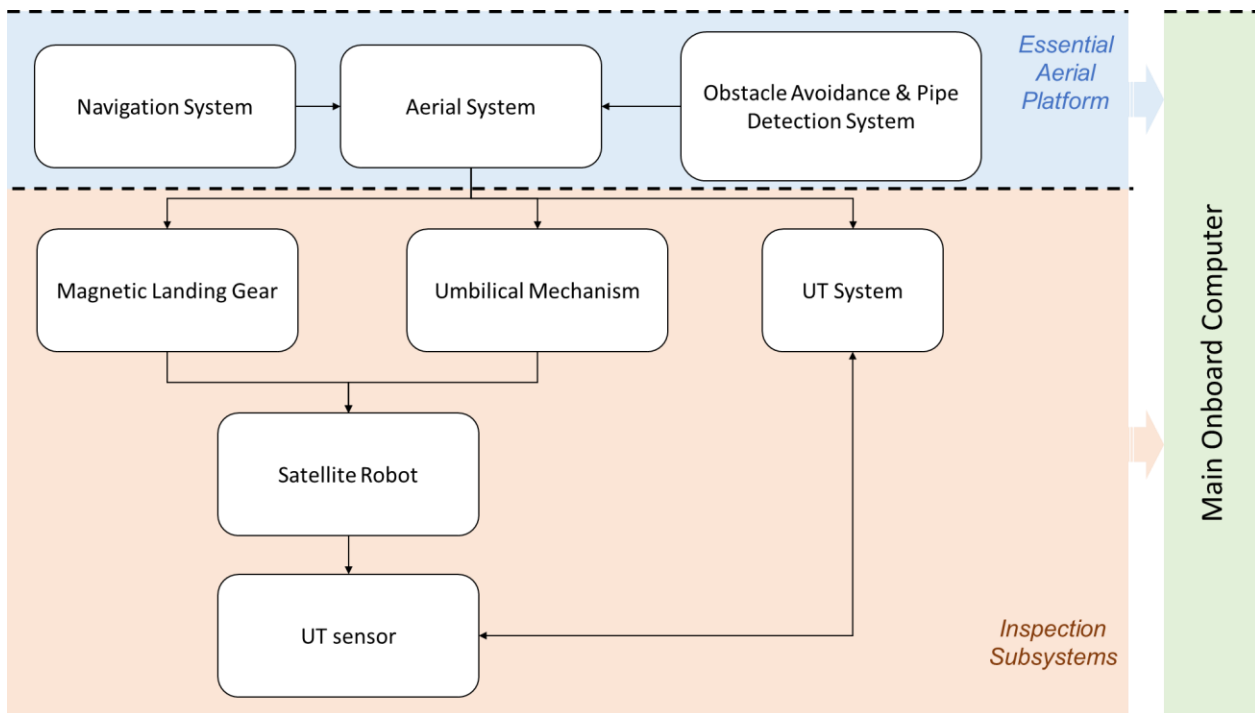
The HMR is composed of an aerial subsystem and a self-propelled semi-independent robotic satellite which has an ultrasonic transducer (UT) roller probe to accomplish the inspection application. Both subsystems have been designed with different but complementary functionalities to meet the requirements of the end-users.

Figure 1 and Figure 2 show the physical subsystems of the HMR and illustrate their hierarchy. The HMR can be decomposed in two main subsystems, the essential aerial platform, and the inspection subsystem. Those can be also split themselves.



**Figure 1 HMR overview.**

Figure 1 shows that as part of the essential aerial platform, we can find the actual aerial system (AP, airframe, propulsive system...), the localization, the obstacle avoidance, and the pipe detection systems. All those components are in charge of guaranteeing the safe behaviour of the aerial robot while flying. Figure 2 also shows that the inspection subsystem is composed by the new concept of magnetic landing gear, the umbilical mechanism, the UT system, and the satellite robot. This part of the HMR is involved on gathering the inspection data while accomplishing the inspection action. All the software except the low-level attitude controller of the aerial system is executed in the main onboard computer through different interfaces. The software integration is clearly detailed in the deliverable D5.2.



**Figure 2 HMR system architecture.**

The following sections describe how the final version of the HMR integrates those subsystems to accomplish their functionalities from the hardware level point of view.

### 2.1. Aerial System

The aerial system that composes the HMR was previously presented in the D2.2 (see Figure 3). During the integration phase, this component has not significantly changed. Along with the WP5, the system was tested in an outdoor controlled environment that emulates the actual use case. We refer the reader to the previous deliverable (D2.2) for more details.



**Figure 3. Final prototype of the HMR robot.**



## 2.2. Final integrated localisation and obstacle avoidance system

As already mentioned in previous deliverables, several cameras are used for the localisation and obstacle detection tasks. In the final version of the HMR, the localization and the obstacle avoidance system are composed of three cameras each one.

The localization system fuses the information provided by three Intel RealSense T265 tracking cameras in a redundant Kalman filter developed in the context of the HYFLIERS project [1]. Two of those cameras are located on the sides of the aircraft wide to the frame by means of the use of dampers, and the third is in the outer ring looking towards the rear of the aircraft as presented in the Figure 4 and Figure 5. With this layout, we pretend to enrich the coverage and visual information perceived by the internal visual simultaneous localisation and mapping (VSLAM) algorithm and avoid pointing a single direction. In addition, those tracking cameras that are in the frame have an angle of inclination of 45 degrees to focus the field of view of the camera on the obstacle-free zone between the rotors and the landing gear.

The obstacle detection component uses three additional depth cameras (Intel RealSense D435) to detect obstacles in the allowed movements of the robot (forward, upward, downward). These cameras provide a dense point cloud of the environment. Additionally, the downward camera is performing the pipe segmentation when required. Those cameras are also helping the controller to decrease the control efforts due they are specifically located in the outer ring of the aerial system to keep centred the centre of mass. Figure 6 shows in detail the position depth cameras, where the new mounting system with dampers can be observed.

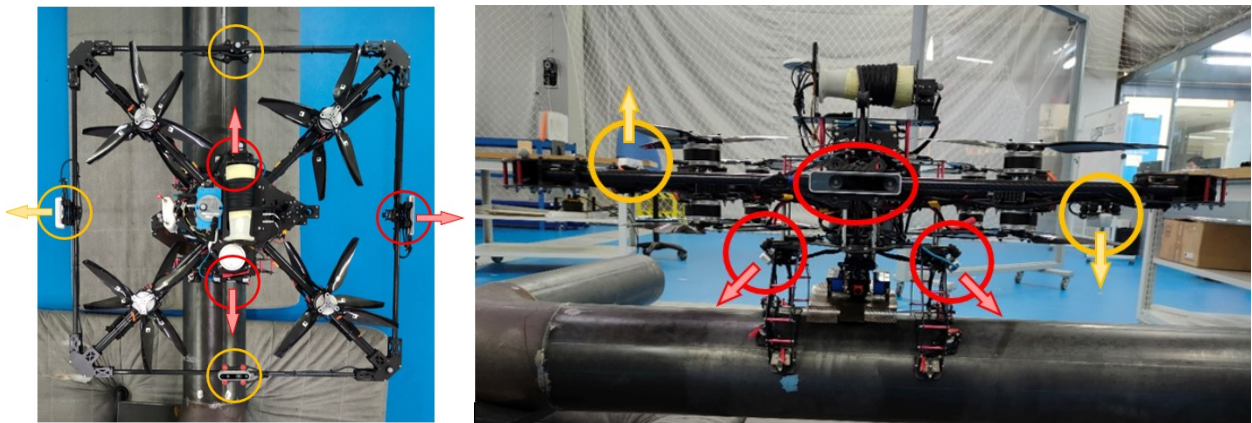


Figure 4 Final cameras position.

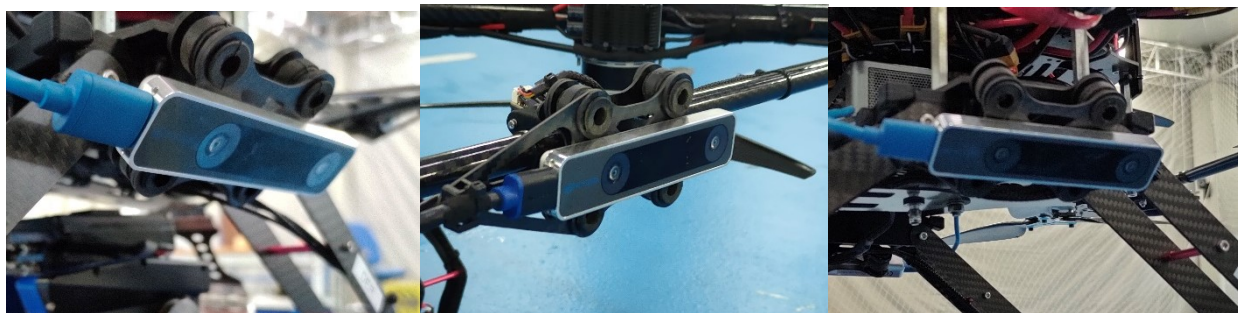


Figure 5 Final mounting system of the tracking cameras shown in detail.



**Figure 6 Final position of the depth cameras shown in detail.**

### 2.3. Ultrasonic System

The following Figure 7 shows the final placement of the ultrasonic electronics on the drone. The location of the UT unit was chosen from the point of view of being as far away as possible from the noise sources (motors, switching power supply, etc). Regarding the length of the transducer cables, which can affect the UT signals, it was decided to incorporate a preamplifier inside the crawler to minimize noise, eliminating the noise figure produced by the length of the cables.

The entire unit can be easily removed since it has a total five connectors; all of them are vibration-proof connectors.

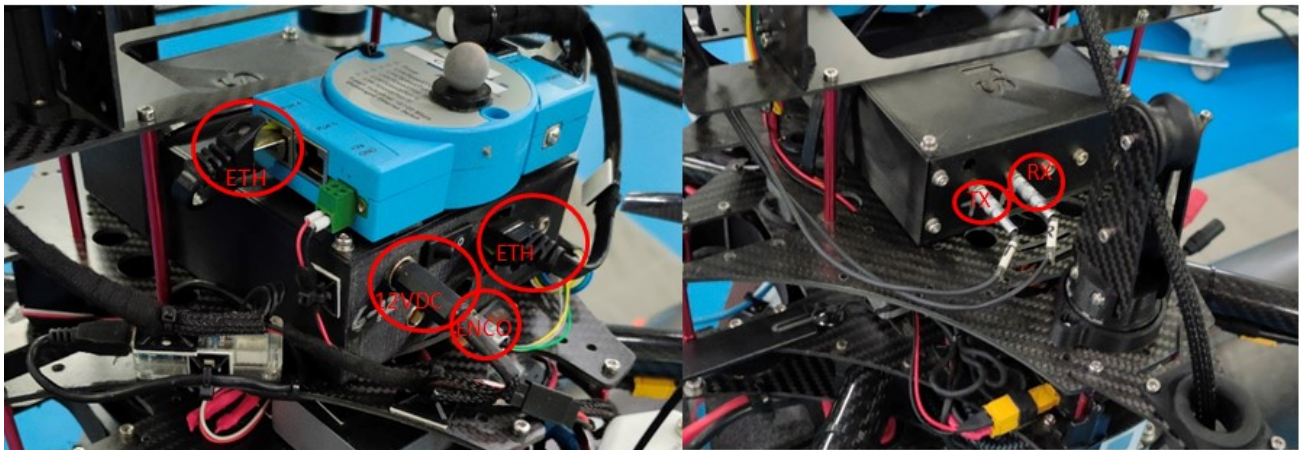


**Figure 7 UT unit installed on the drone.**

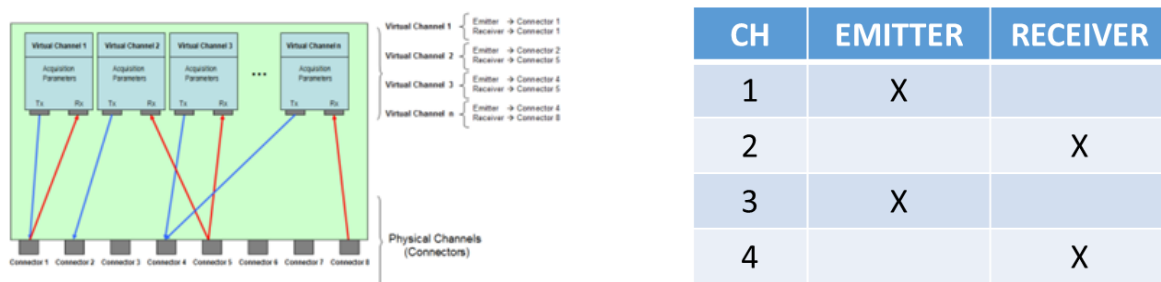
As it is shown in Figure 7, the UT system is composed of an ETH switch which establishes the connection between the UT system and the ground control station (GCS) through the wireless link. A quadrature encoder attached to the rolling probe to allow the synchronization of the UR signal with the mechanical movement of the UT rolling probe. A battery that supplies the UT unit in a range between 6-12 V and 0.8 A. And last, the UT rolling probe, which is a transducer connected to the UT unit through a RG54 coaxial cable with the Lemo00 standard.

Table 1 summarizes the main characteristics of the ultrasound unit mounted on the HMM which was selected according to the specification collected in the document D1.4.

**Table 1 Main Characteristic UT unit table**

<b>Power consumption</b>	7 W max = 1100 mA (6 V), Loaded 50 $\Omega$ , PRF=5 KHz, pulse amplitude -400 V.
<b>Power supply</b>	6/12/ 24 Volt @ 0,8 Ampere
<b>Temperature range</b>	0 °C to 50 °C (Ambient)
<b>Operative system</b>	Microsoft Windows 32/64 bits 7, 10/ VISTA / XP / 2000 / 98SE
<b>Communication</b>	150 Mbs Wireless Ethernet TCP/IP y UDP/IP. Data Rate: >7 Mbyte/s. Frequency Band 2.4~2.4835GHz Radio Data Rate 11n : up to 150Mbps (Automatic) 11g : 54/48/36/24/18/12/9/6M (Automatic) 11b : 11/5.5/2/1M (Automatic) Frequency Expansion DSSS(Direct Sequence Spread Spectrum) Modulation DBPSK, DQPSK, CCK, 16-QAM, 64-QAM, BPSK, QPSK Security 64/128/152-bit WEP, WPA/WPA2, WPA2-PSK/WPA-PSK Sensitivity @PER 135M: -70dBm@10% PER 65M: -73dBm@10% PER 54M: -76dBm@10% PER Mode AP Mode, Router Mode, Repeater Mode, Bridge Mode, Client Mode
<b>Internal Memory</b>	48 MB (24 Mega-Samples)
<b>Size</b>	160 mmx 110 mm x 35 mm
<b>Weight</b>	300 Grams
<b>Ut Channels</b>	4
<b>Encoder</b>	2 ( differential)

The HYFLIERS UT system has been configured for 1 to 4 physical multiplexed channels. These ultrasound channels can be configured as emitter, receiver or emitter and receiver. The user program an acquisition sequence with up to 32 virtual channels, these virtual channels are defined assigning one connector for emission of the pulse and other connector (or the same) for reception of the signal, and it is possible to share connectors between virtual channels. Figure 8 shows the configuration have selected as we describe in the table of Figure 8, as the rolling probe has 2 transducers, we use only CH1 & CH2.

**Figure 8 Channel configuration.**

Moreover, during the integration process, some new modification had to be made in the ultrasound unit,

- **Encoders:** 4 pull up resistors are mounted for Encoders A and B. The pull up resistor is 2k7 and they are mounted between signals A+ and B+ of the encoders (pins 3 and 5) and the VPD\_F power supply line of the Encoder (Figure 9).





Figure 9 PULLUP resistor encoder.

- **Improve the Bandwidth:** To improve the bandwidth of the UT unit we have changed the value of C62 from 68pF to 47pF. (It is modified in the design). This has been detected in the initial inspection test, with this modification we improve the axial resolution 12%.

Table 2 New BandWidth of the UT unit: a) Low frequency, b) High frequency

Channel	Signal		Amplitude		Cutt-Off	Frequency
Ch 1	325,0 mVpp	0,2 dB	58,2 %	-2,8 dB	-3,0 dB	981 KHz
Ch 2	325,0 mVpp	0,2 dB	57,5 %	-2,8 dB	-3,0 dB	1022 KHz
Ch 3	325,0 mVpp	0,2 dB	58,6 %	-2,8 dB	-3,0 dB	953 KHz
Ch 4	325,0 mVpp	0,2 dB	57,5 %	-2,8 dB	-3,0 dB	1028 KHz
Ch 5						
Ch 6						
Ch 7						
Ch 8						

Channel	Signal		Amplitude		Cutt-Off	Frequency
Ch 1	172,0 mVpp	-5,3 dB	30,8 %	-8,3 dB	-3,0 dB	24100 KHz
Ch 2	178,0 mVpp	-5,0 dB	31,5 %	-8,0 dB	-3,0 dB	24400 KHz
Ch 3	172,0 mVpp	-5,3 dB	31,0 %	-8,3 dB	-3,0 dB	24600 KHz
Ch 4	172,0 mVpp	-5,3 dB	30,4 %	-8,3 dB	-3,0 dB	24830 KHz
Ch 5						
Ch 6						
Ch 7						
Ch 8						

- **Encoder cable short circuit prevention:** To prevent short circuit from the encoder's robot (wiring problems), a 5V linear regulator (L4941BV) is mounted between the 12V power input and the encoders power supply. Fuse F1 has been removed so that the Encoder is not powered by the 5V source (VPS) of the UT units. Mounted a linear regulator as shown in the picture, putting a 0.5A resettable fuse in series with the regulator input and mounting a 47μF 6.3V SMD 1206 capacitor between the regulator output and GND.



Figure 10 Encoder cable short circuit prevention.

- **Extension of the power supply range of the UT unit:** Because the drone has a standardized power supply (12 Volt), the UT unit which normally operates at 6 Volt, was modified, expanding the range to 12 Volt. On the other hand, a circuit that prevents polarity inversion is incorporated in the integration process.

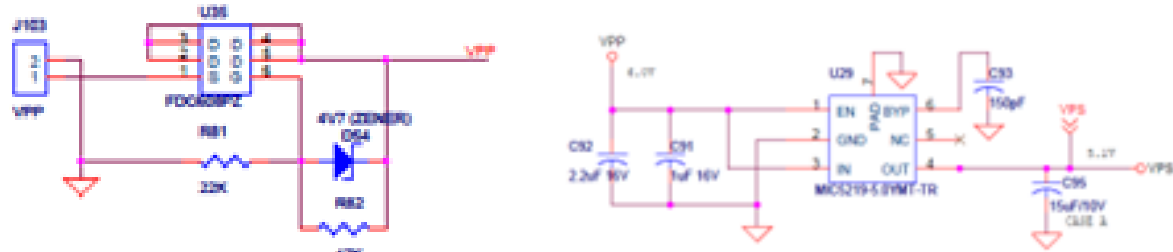


**Figure 11** Circuits to prevent the polarity inversion (left) and to extend power supply range (right).

## 2.4. Integrated satellite robot

The satellite robot capable of magnetically crawling along a magnetic pipe as shown in Figure 12 is integrated with the drone to together form the hybrid system. Jointly they implement the remote ultrasonic inspection capabilities demanded by the use-case.

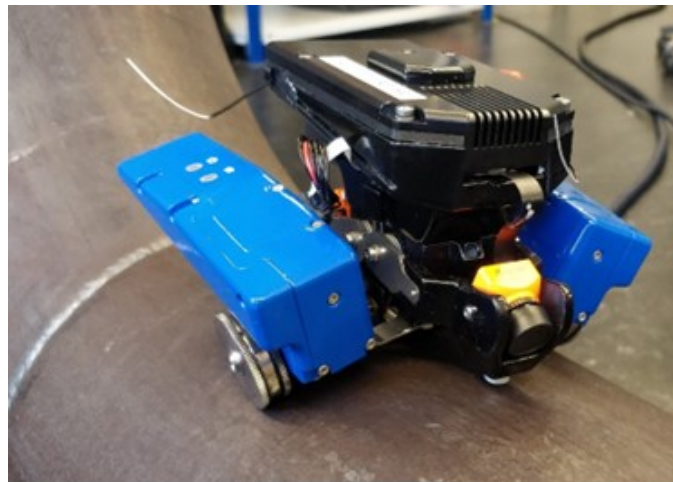


**Figure 12** HMR satellite.

Power supply is provided from the battery on the flyer through an umbilical between the two. Two coax signal cables connect the ultrasonic sensor on the satellite to the UT instrument on the drone. Additionally, an incremental encoder signal is provided from the satellite to the UT instrument to match measurement signals to relative position values. This enables the recordings of accurate B-Scans (line measurements).

Controls for this crawler are directly connected to the ground control station through two dedicated radio links for movement and camera feed. A handheld RC controller and video display allows the pilot to control and remotely monitor the robot even when no direct line of sight is possible. Figure 13 shows the satellite close to a weld on a pipe and the corresponding camera feed that is displayed to the pilot.



**Figure 13 Satellite camera and feed.**

The ultrasonic probe is mounted at the belly of the satellite. The kinematics of the crawler is specifically designed to ensure the crucial perpendicular orientation of the ultrasound beam to the surface to be inspected. Silicon oil is used as couplant to conduct the ultrasonic wave between the sensor and the pipe. This type of fluid is chosen due to its chemical compatibility with the rubber tire material of the probe. A small reservoir above the probe continuously applies a fresh film onto the contact surface. In combination with the flexible tire of the probe allows for long inspection distances without having to refill the couplant. When the HMR is landed at the ground control station, the reservoir can be replenished using a syringe as shown in Figure 14.

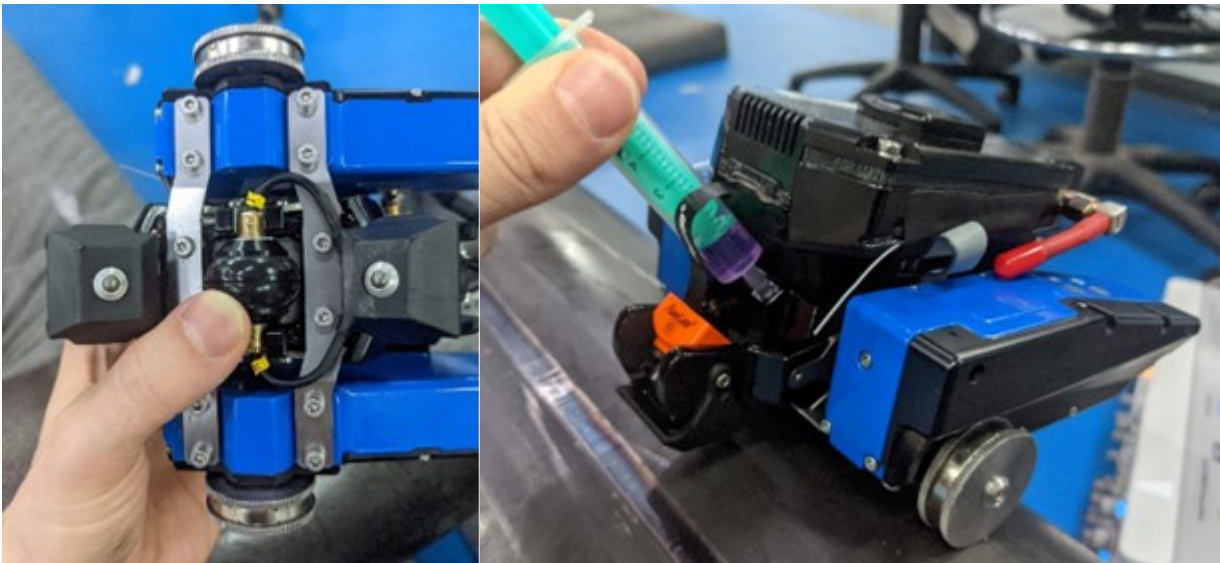


**Figure 14 Inspection sensor and couplant management.**

Due to high attenuation, the chosen sensor and the cable length between satellite and instrument, a preamplifier designed by DASEL has been integrated into the Satellite. It boosts the weak return signal from the ultrasonic sensor before going through the ~3.5-meter cable to the UT instrument on the drone. It is supplied with power from the central connector board.

The final integrated system can be used to perform fully remote-controlled ultrasonic inspection of the targeted process piping. Once the drone is landed and the satellite deployed, the pilot can use the cameras to guide the unit to a known reference location like a weld. From there the desired starting location can be accurately pinpointed by using the incremental encoder feed accessible through the



ultrasonic analysis software. Point and line scans in the quadrant locations along the pipe as depicted in Figure 15 are performed to assess the remaining wall thickness of the asset.

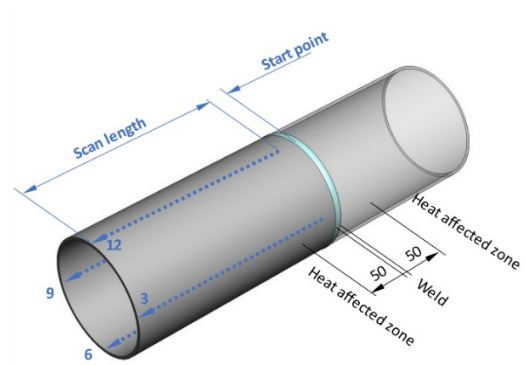


**Figure 15 Performing a longitudinal line scan on a straight pipe section.**

### 2.5. Magnetic Landing Gear for non-insulated pipes

The following images show the final assembly of the landing gear together with the crawler according to the design presented in the D2.2.

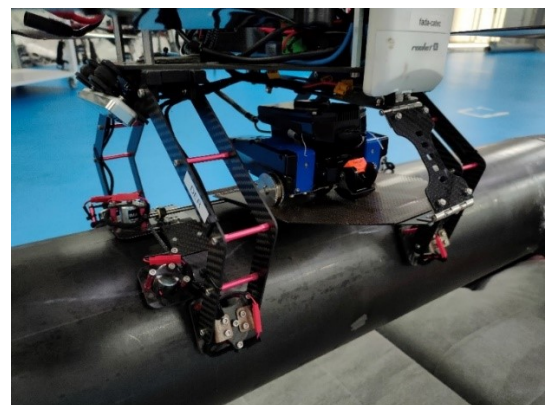
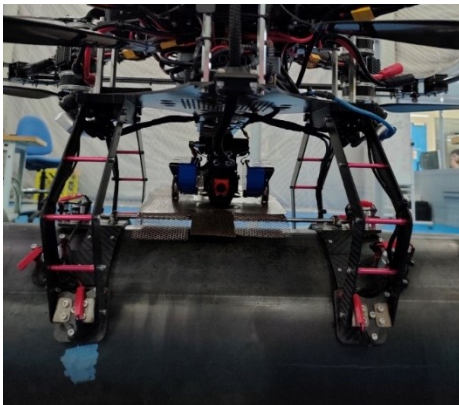


**Figure 16 Final landing gear.**

The following picture shows the location of the magnets on the undercarriage and the adjustment of the magnets on the pipe, achieving a better adherence to the surface.

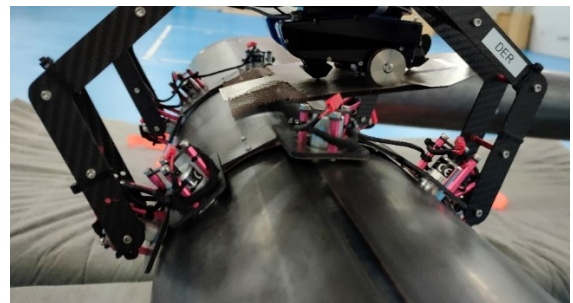
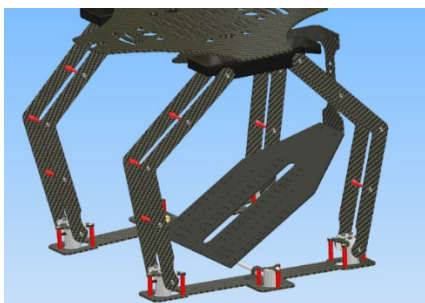


**Figure 17 Landing gear magnets design and “as built” shown in detail.**

The magnetic landing gear has been successfully tested in pipes of 12, 8 and 6 inches.

The joint between the aerial system and the magnetic landing gear is done through a passive DoF, to facilitate the accommodation of the aerial robot once landed. This avoids having an extreme rigidity in the contact phase that could lead to an undesirable and unsafe behaviour and keep the aerial system horizontal even if the robot does not land over the centre of the pipe.

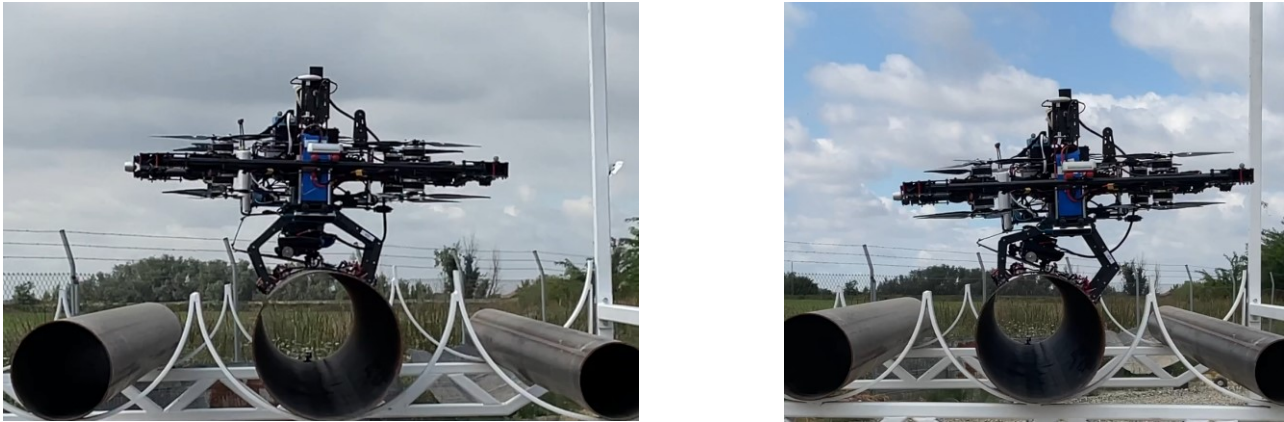


**Figure 18 Landing gear magnets shown in detail.**

## **2.6. Umbilical Mechanism**

The following pictures show the umbilical mechanism to roll up the umbilical cable of the crawler.

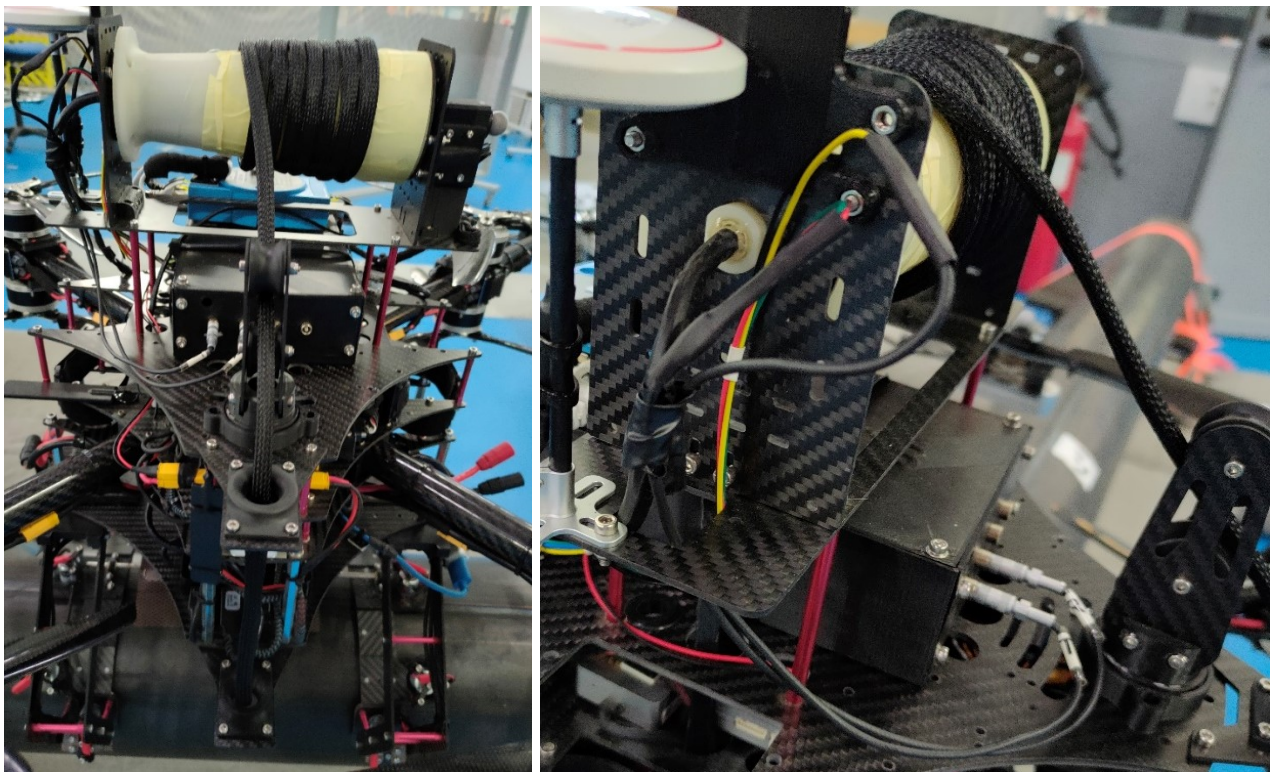


**Figure 19 Cable rolling final system**

Figure 20 shows the umbilical mechanism during its operation when the crawler is moving.



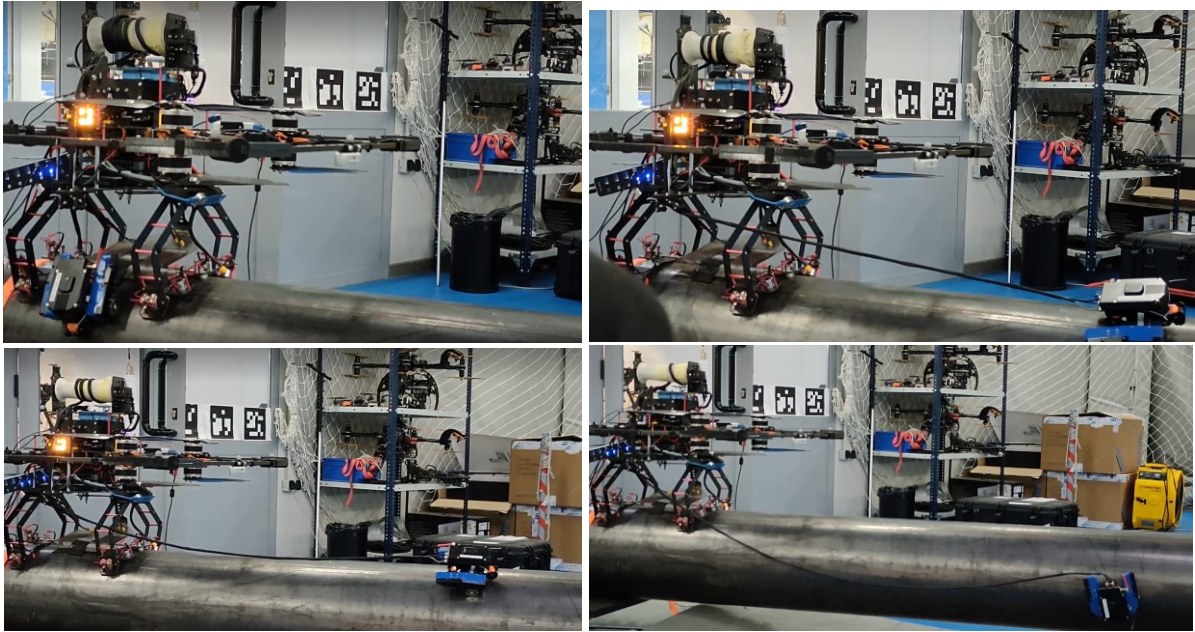


**Figure 20 Slipping used for the cable rolling movement.**

## 2.7. General connections and communications

For ground communication, the bullet was replaced by an Ubiquiti AC to increase the robustness and the range of the wireless link. The following image shows the new component installed in the drone as well as the new network architecture.

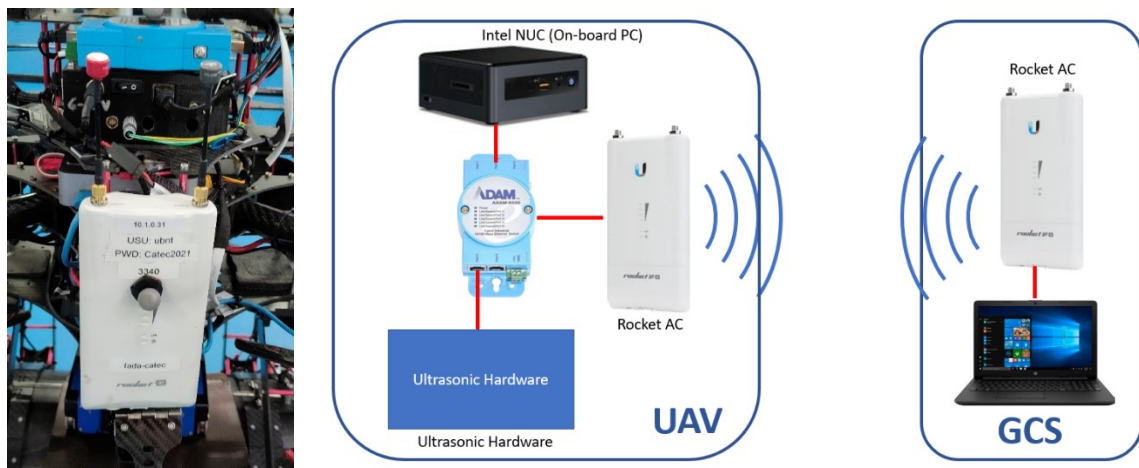


**Figure 21 Ubiquiti AC mounted in the drone and network architecture.**

### 3. HRA final prototype

The Hybrid Robot with Arm (HRA) consists of a hybrid robot which can fly, land on the pipe and crawl over the pipe while the inspection is being accomplished. The final design has been derived from the experience of the previous designs presented in deliverable D2.1 and the experiments performed with them.

As in the previously mentioned HMR, Figure 22 and Figure 23 show the physical subsystems of the HRA and illustrate their hierarchy. The HRA can be decomposed in two main subsystems, the essential aerial platform, and the inspection subsystem. Those can be also split themselves.

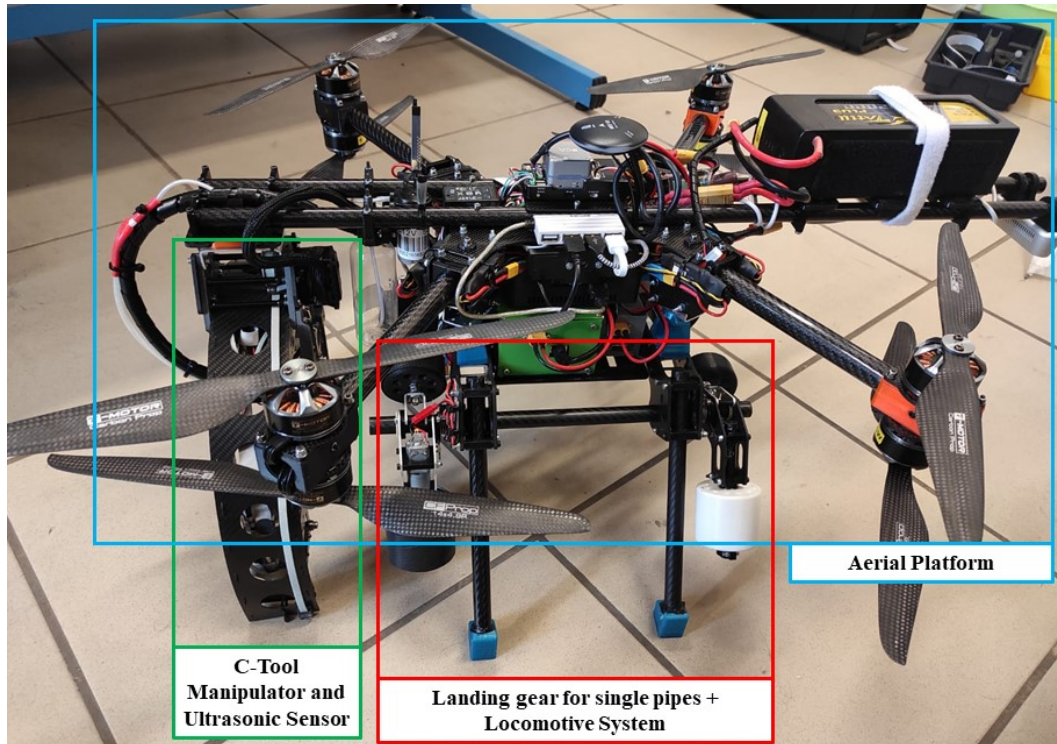


**Figure 22 Main hardware subsystems of the HRA.**

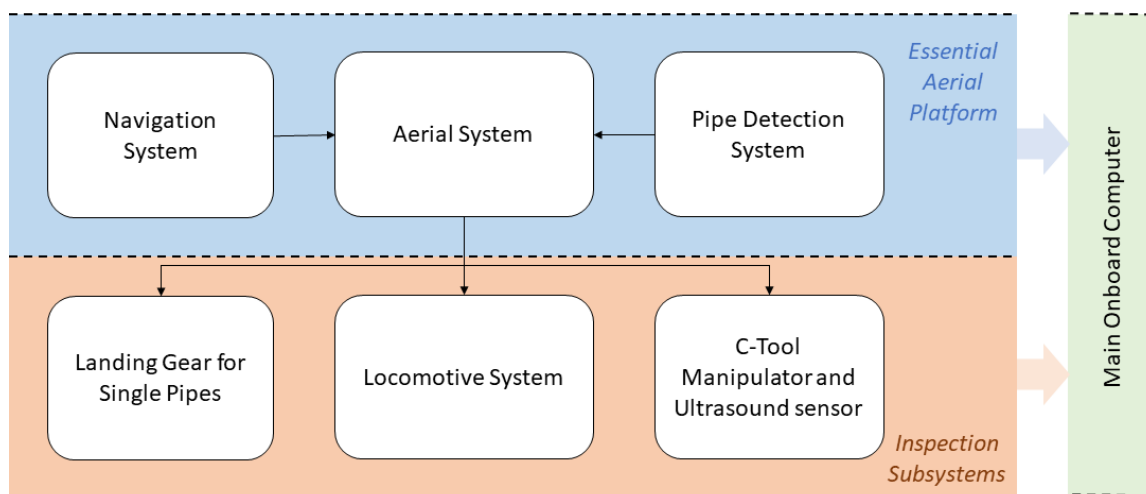


**Figure 23 Systems hierarchy of the HRA.**

The aerial robot has been designed to fulfil the size limit needed to fly and operate in the congested environment of a refinery, with the specifications defined in D2.1, having a required maximum overall diameter (tip to tip) of 1 m, and a maximum take-off weight (MTOW) of less than 9 kg with a payload for the tool of 1,5 kg.

The final aerial platform has been redesigned to be able to cope with larger payload. From the different add-ons described in D2.1, the HRA final prototype implements the landing gear for single pipes, with a new design with passive wheels and a torsion spring to attach to the pipe, and active wheels to move along the pipe.

### 3.1. HRA final aerial platform



**Figure 24 HRA final aerial platform overview (without propellers).**

The final aerial platform of the HRA is shown in the Figure 24. All of its hardware specifications, materials used and some design details can be found documented in D2.2.

Regarding electronics, the aerial platform mounts a Cuav V5+ autopilot running PX4 firmware. A PW-LINK Wi-Fi Radio provides telemetry from the autopilot to the GCS. A BEC provides power to autopilot from the main battery. A safety switch is also included.

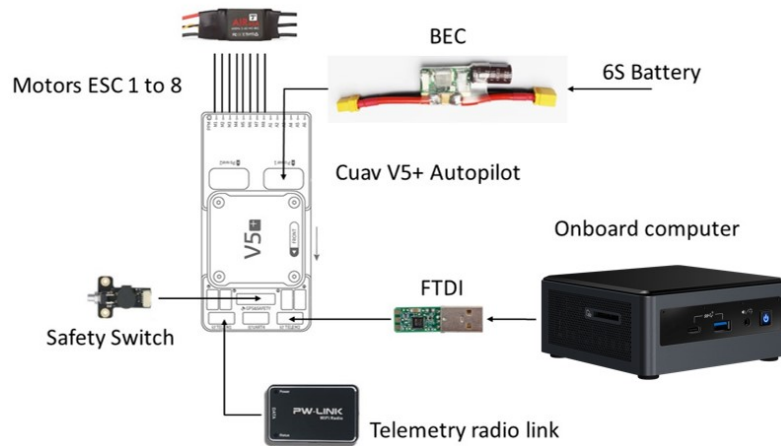
On top of that, an onboard computer must be included to provide the functionalities related to the autonomous operation of the aerial robot. These functionalities are:

- Position estimation.
- Mission control.
- Landing coordinated control.
- C-tool control.
- Control of movement along the pipe.



The onboard computer is connected to the TELEM2 port of the autopilot through an FTDI TTL Converter for communication. The onboard computer and the Ground Station work in the same Wi-Fi network.

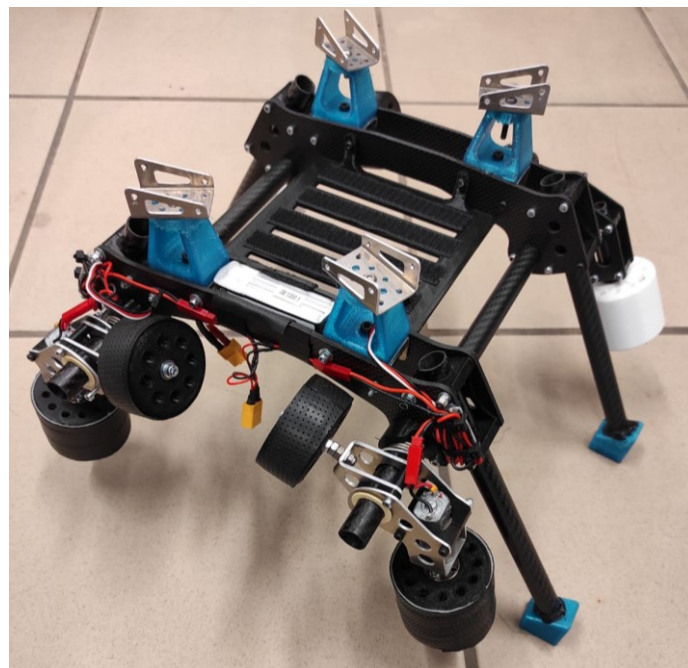
The electronics wiring scheme is shown in Figure 25.



**Figure 25 Autopilot and onboard computer wiring scheme.**

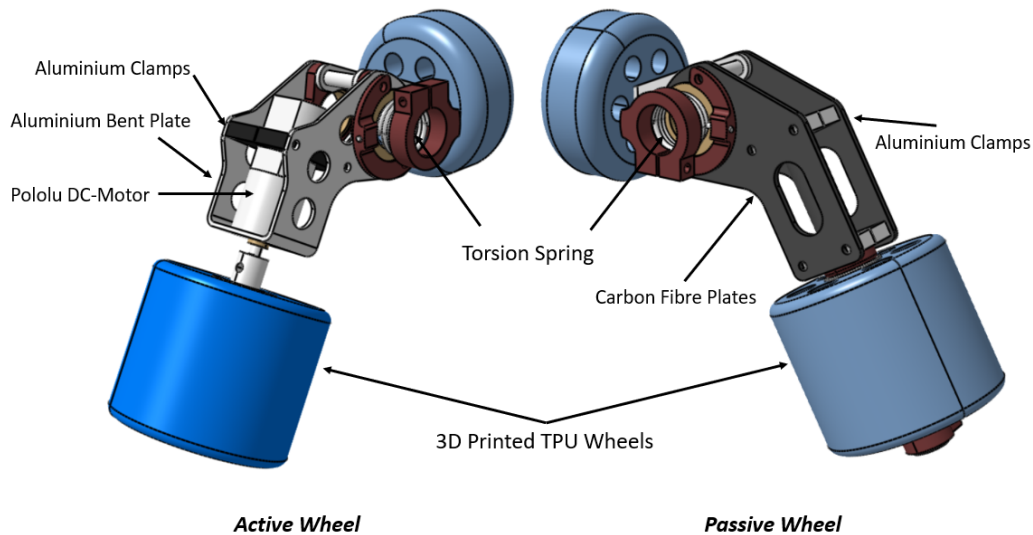
### 3.2. Final landing gear for single pipes

Figure 26 shows the final setup of the HRA landing gear for single pipes. It consists of four carbon fibre tubes that allow the platform to land properly. These four tubes are attached to four vertical carbon fibre plates by means of aluminium clamps. Apart from the main carbon fibre structure, four-wheel systems have been included in the front and rear plane of the landing gear.



**Figure 26 Final landing gear for single pipes.**

Figure 27 includes details of both active and passive wheel systems. A torsion spring allows the wheels to open when the octocopter needs to leave the pipe once the mission is completed.



**Figure 27** Wheel systems for the final landing gear.

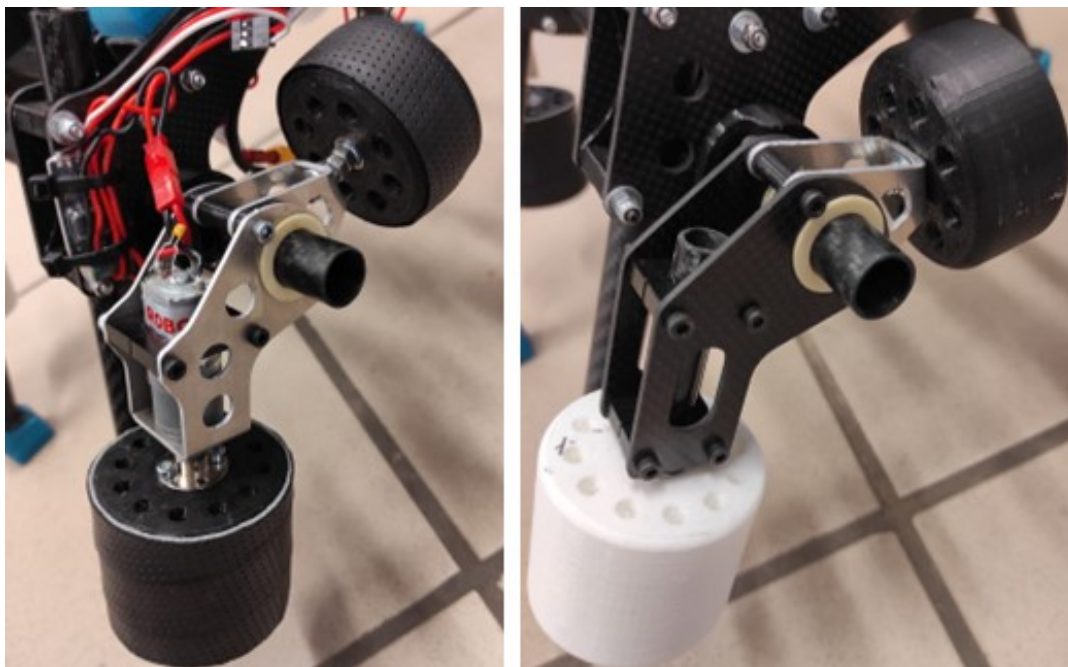


**Figure 28** Active (left) and passive (right) wheels for the final landing gear.

### 3.3. Integrated HRA C-tool manipulator and ultrasonic sensor

The HRA prototype uses a tool specifically designed to perform thickness inspection of 8-inches pipes. The tool is shaped with a C form suitable for wrapping the pipe surface, sliding on it to have complete map a its internal thickness.

The primary innovation of this tool with respect to other technologies is that our device can completely wrap the pipe, rotating around its central point (See Figure 29). In this way, the complete surface of the pipe section can be quickly inspected. The measuring tool is endowed with a Degree of Freedom designed to allow the rotation around the pipe axis. A complete rotation of 180 degree is allowed ( $\pm 90$  degrees in clockwise and counter-clockwise directions). Such rotation is fundamental to reach also the bottom side of the pipe. To perform the thickness measurement and facilitate the

integration the tool was equipped with two ultrasonic probes, provided by Tritex NDT device. These probes require for a coupling liquid to properly perform the measurement. In this tool, we rely on simple water as coupling liquid transferred on the pipe, we rely on a set of wet sponges to put some water on the inspecting surface before get the measurement. For this reason, a water pump wetting two sponges closer the tritex probes are considered.

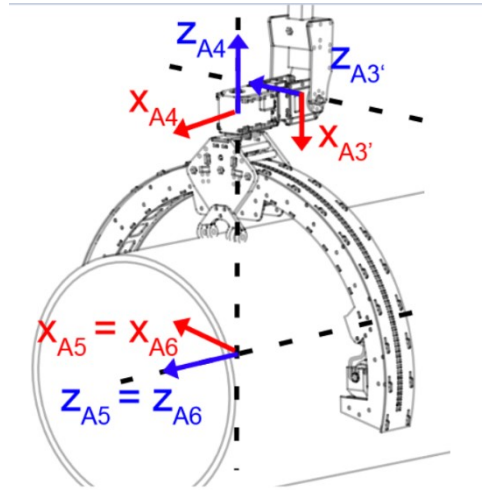


**Figure 29 Kinematic frame of the C-Tool. A5 represents the rotation frame of the tool.**

An overview of the whole hardware of the C-Tool is reported in the following figures.

1. The electronics external to the C-Tool is boxed in two lightweight boxes containing a microcontroller that interface the C-Tool with the high-level computer (in our setup an intel up squared) and a box containing the Tritex NDT inspection Tool, a shown in Figure 2.

The Tritex device (grey box in Figure 30), communicates with the external onboard computer with an USB/Serial cable and is connected with the two probes attached to the C-Tool frame. Differently, the green box of Figure 2 contains the main controller element of the tool that is represented by an ST Nucleo f767ZI microcontroller. This device communicates with the onboard computer with a local network interface, while is connected to the tool via i2C and serial connections. The role of this device is to control the Dynamixel motors of the tool and control the second micro controller placed directly on the tool chassis.

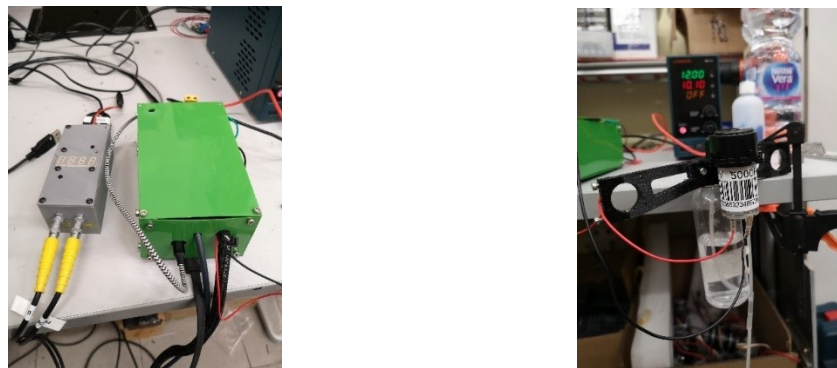


**Figure 30 (Left) C-Tool electronics (Right) C-Tool water pump.**



2. In Figure 31, the water pump used to wet the inspection surface is depicted. It is represented by a water contained with two cables attached to the Tritex probes. An electro valve is used to push the water liquid towards the probes.



**Figure 31 C-Tool over the pipe**

The measuring tool is depicted in Figure 3. It is versatile and can be equipped with different thickness probes to inspect the pipe sections. It is composed of a semi-circular ring able to slip under a circular path with respect to a cart fixed on the last arm link (see Figure 29).

The tool ring is composed of three carbon plates of 1 mm each. One of these plates is curved externally while the other two are stuck through several teeth to form a unique rigid structure. The fixed cart is endowed with several rolling bearings on the guide defined by the three-carbon plates of the tool. A belt-pulley mechanism controls the motion of the tool along its tangential direction (i.e. the rotation of the two extremities of the tool with respect to the pipe axis). The extremities of the tool mount two thickness probes to measure the whole pipe circumference, as shown in Figure 31.

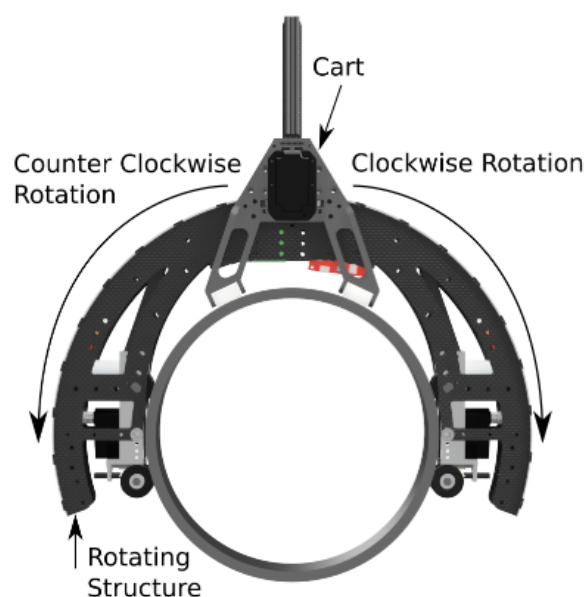


**Figure 32 C-Tool: front view.**

Among the different ultrasonic sensors that can be added to the designed tool, in our setup, we used two single-channel Tritex probes are used. To have good measures, it's important to fix these probes upon the surface. A clamping mechanism has been designed to perform the following operations:

- Detaching: this operation is needed to move the manipulator towards another section to inspect. This operation is depicted in Figure 33.

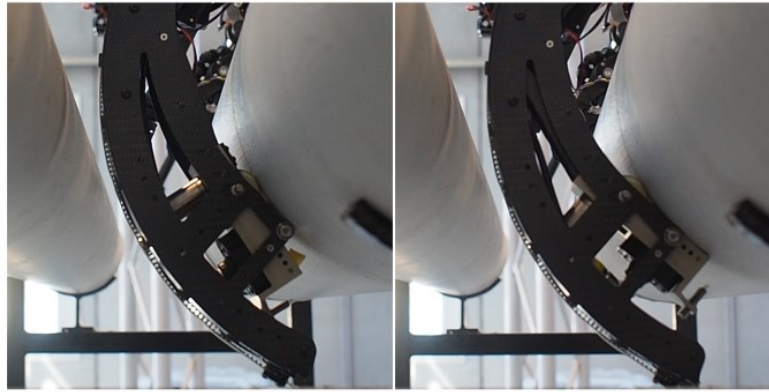


**Figure 33 Detaching mechanism to perform the thickness measurement.**

- Rolling: the probes around the pipe circumference to perform the thickness measurements of a specific section, overcoming the high friction generated by the magnetic forces.

These operations are allowed by the C-Tool mechanisms. In particular, two compact carts with four rubber each (two on the top and two on the bottom of each cart) allow the execution of these operations, implementing the detaching and rolling mechanisms. This design is depicted in Figure 34.

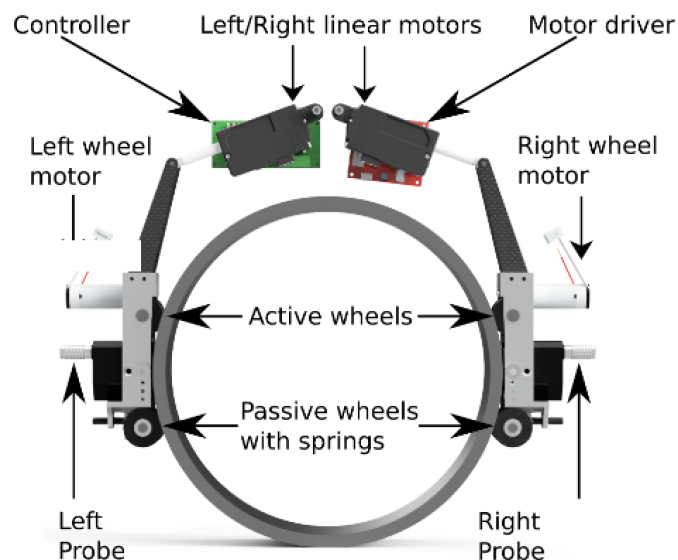


**Figure 34 C-Tool: internal components.**

The motor torque has been calculated by evaluating the static magnet friction of the probes experimentally when attached to the pipe to be 24 N. Hence, the torque required to slither the tool around the pipe has been calculated considering the radius of the active wheels and dividing the torque

equally to the two motors ( $\tau_w = 0.12$  Nm torque needed). So, the required torque to the motors is  $\tau_m = \tau_w/K = 0.004$  Nm. Differently, the wheels placed on the bottom side of the carts are passive and are attached to a miniaturized linear guide pushing towards the tube by two screws with an integrated spring. This solution allows to regulate the force that the two bottom wheels exert against the pipe. As for the detaching mechanism, the two carts can rotate around the axis of the cartwheels in order to detach the probes from the pipe. In particular, when the tool needs to be moved from its current position (i.e. folded or moved to another section of the duct), a couple of linear motors pull the probes to detach them from the ferromagnetic surface. The vice-versa motion procedure is performed to attach the probe to the pipe. This mechanism is better detailed in Figure 35.

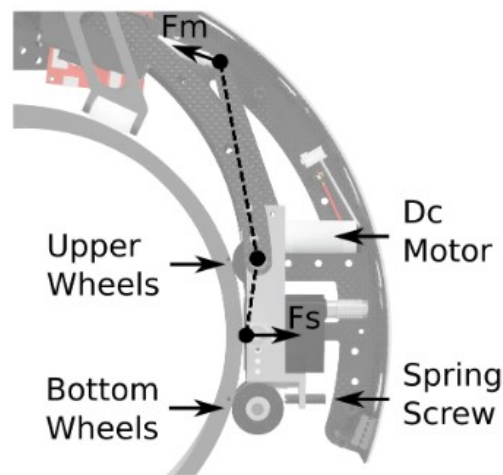


**Figure 35 Tool with EMAT sensors: detail of the EMAT detaching mechanism.**

Each linear motor is able to produce a force of 100 N ( $F_m$ ) that, considering the angle of the applied force and the lever mechanism, is translated in a force of up to 120 N ( $F_s$ ) applied on the axis of each probe in order to detach from the pipe.

As for the system electronics, as already stated the whole tool is controlled using two different micro controllers. In particular two ST micro controllers are used in the following way:

- ST Nucleo f767ZI (Micro1): Controls the rotation around the pipe and sends data to the tool clamps and the active wheels;
- ST Nucleo f3038 (Micro2): Receives control data from Micro1 and directly controls the active wheels and the linear motors to open/close the tool clamps.

### 3.4. Integrated HRA final prototype

The C-Tool has been assembled to the rest of the platform by means of a carbon fibre plate and a TPU damping part in the front area of the whole system. In order to reach a proper mass equilibrium, a 12000 mAh battery has been positioned over the top carbon fibre tubes and rearwards.

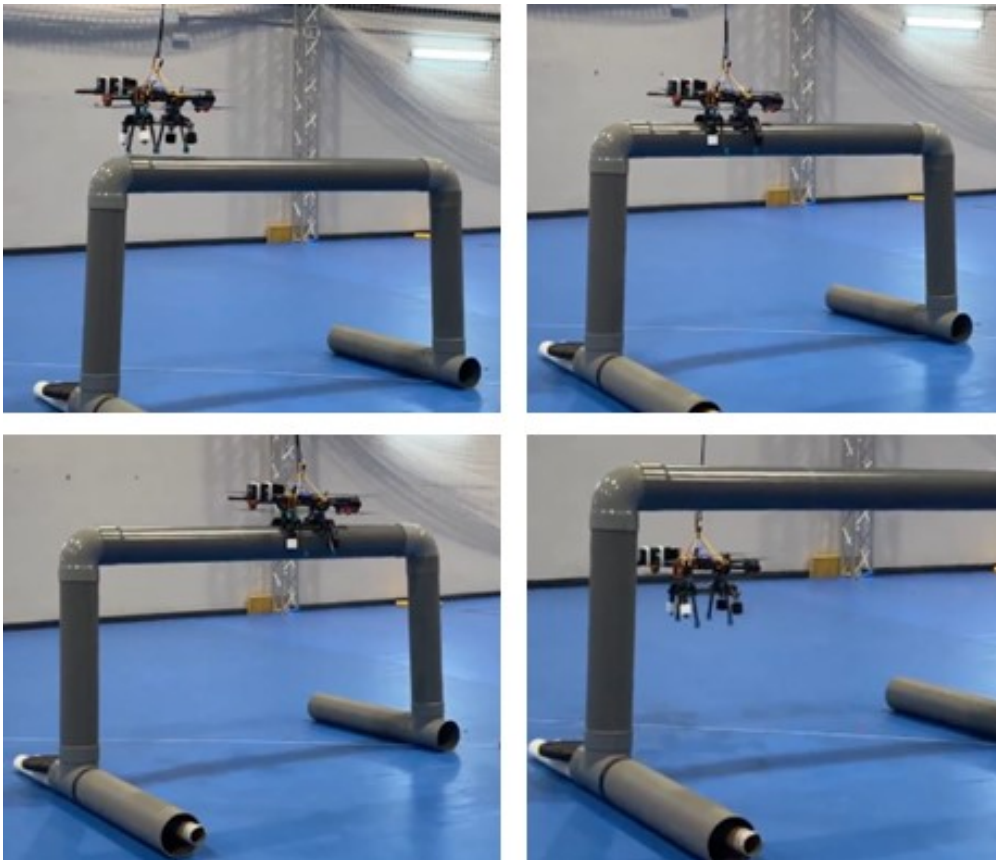
Electronics and Tritex sensor boxes have been placed below the main platform, over a PLA 3D Printed plate.

Figure 36 shows the complete integration of the octorotor platform and the C-Tool.



**Figure 36 Complete integration of the multirotor platform and the C-Tool.**

Figure 37 includes a video sequence of a complete mission performed by the platform. The system takes off, lands on the pipe, crawls and moves forwards, and finally leaves the pipe to land on the ground again. For safety reasons, a rope was attached to the platform in this concrete experiment. However, the rope does not interact with the mission at all.



**Figure 37 Complete video sequence of a mission performed by the platform.**



## 4. Ground segment systems

The ground segment is divided in two different systems, the classical ground control system, and the ground support system. The first one oversees managing and monitoring the mission. It is composed of the control terminal and the UT ground terminal. The control terminal monitors and visualizes the state of the mission from the robotic system point of view. The UT Ground terminal is focused on the proper inspection operations. The ground support system focuses on the additional systems proposed around the HYFLIER operation and it is mounted over a Mobile Support Platform (MSP). A Wi-Fi link realises communication between the HYFLIER's robot (the hybrid robot, HR, represented by either the HMR or the HRA) and ground operators in both systems of the ground segment. The MSP also includes a battery management system to increase the operation efficiency during the test in the field. Together with the ground station database (GSDB) and the inspection engineer user interface (UI), all the above is depicted in Figure 38. The different subsystems of the MSP from a hardware level point of view are described in the following sections. The ground control system are pure software entities and will be described along with the D5.2 in detail.

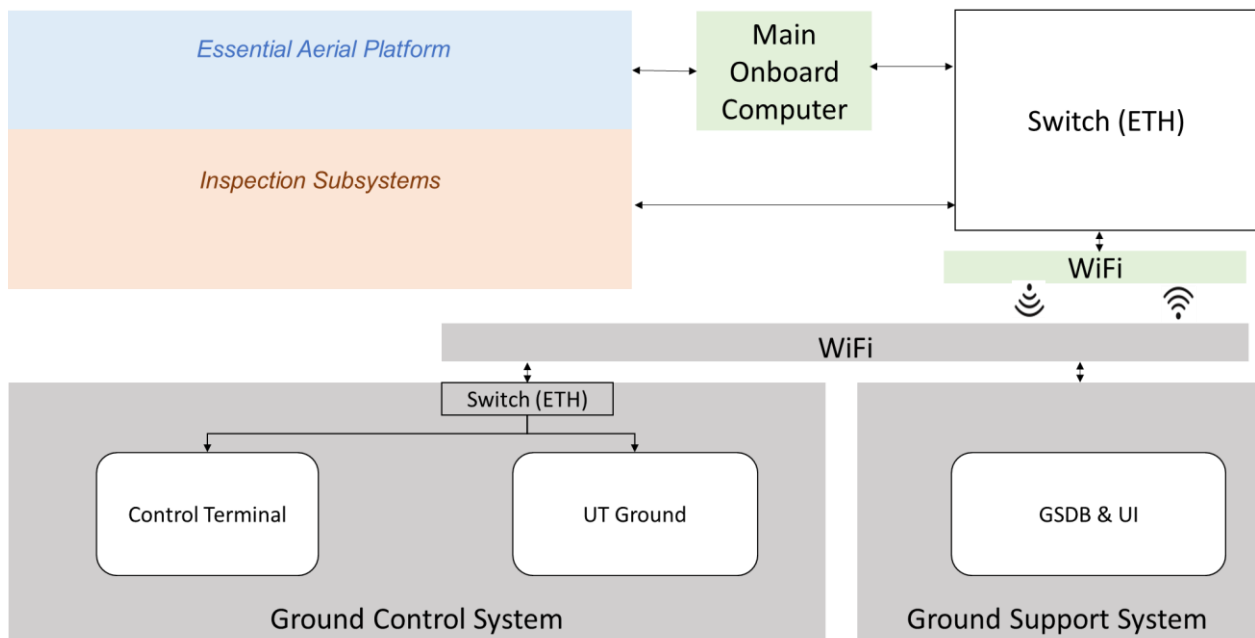


**Figure 38. HYFLIERS global architecture.**

### 4.1. MSP cart System

The support platform is powered by a large main battery, which has been tested with the MSP computer system. The testing configuration of the battery system with the Battery Management System (BMS) module is shown in Figure 39. The battery system is rechargeable currently with an external charger and has connectors for computer power output and for HR charger power output from the main battery. The BMS is currently interfaced with Bluetooth to an Android phone for reading the battery data. The Support PC box is shown in Figure 40 (left).

The cart battery system does not include the custom charger and power-path control board, although the board design has been completed. This is mostly due to longer than expected development time due to pandemic related delays and other problems, and also due to the complexity of the high-power electronics related design issues of the board. The KiCad rendering of the designed board is shown

in Figure 40 (right). The board is designed to facilitate a NUCLEO-F446RE development board for charging & power-path control software development.

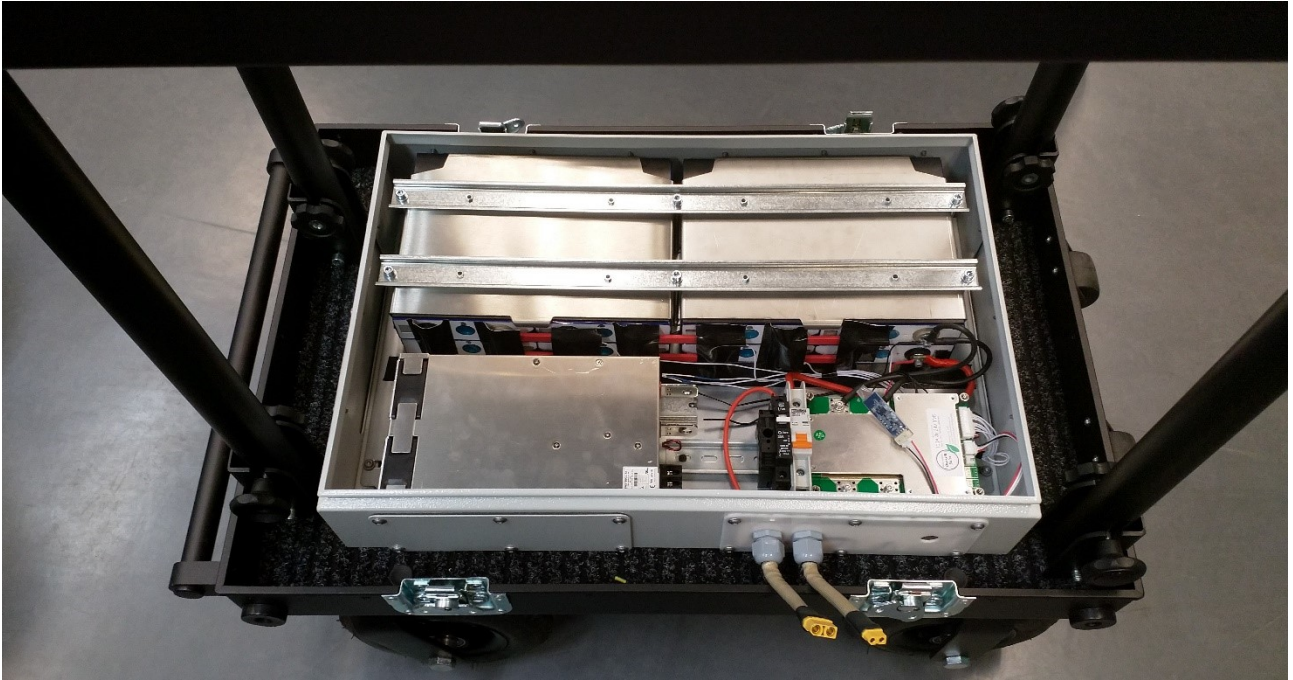


**Figure 39. Implemented MSP main battery system used in functional testing.**

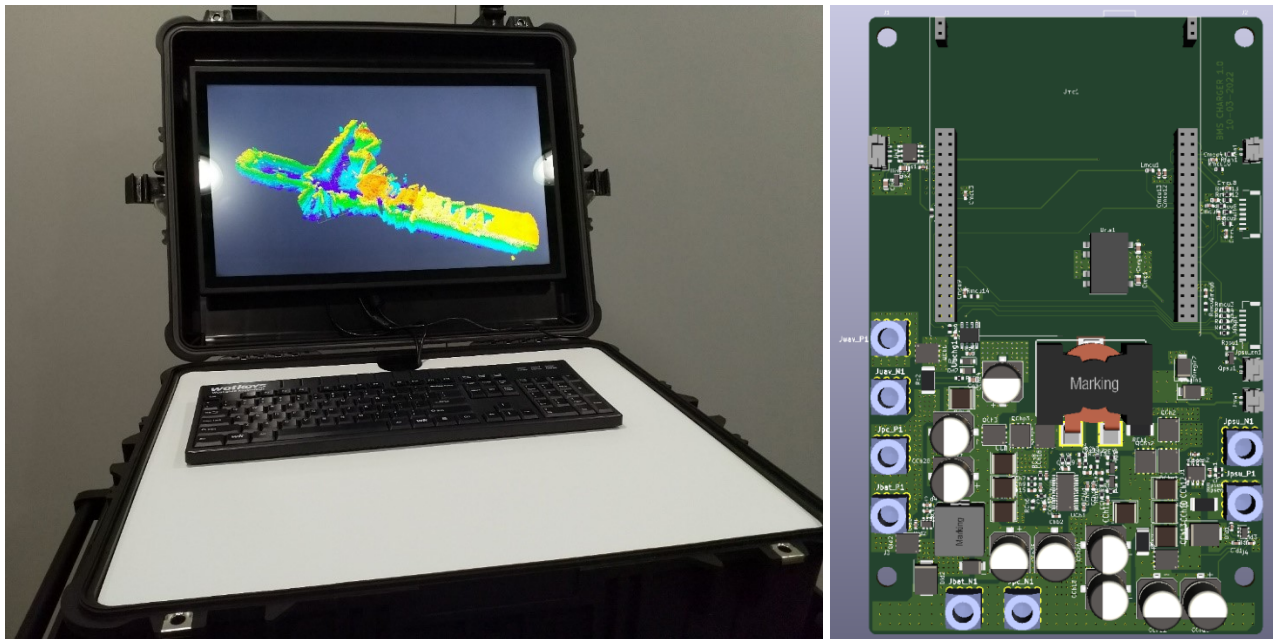


**Figure 40. Left: MSP Support computer box. Right: Custom battery charging and power-path control board.**

## 4.2. MSP Support Computer

The MSP support computer with ROS related functions and the wireless network has been tested and have been used in development of robot navigation related tasks. ORB-SLAM2 based localization and basic route generation has been tested on the MSP computer using ROS Melodic Morenia. For

some more development, they could be used as support function for path planning and navigation. ROS nodes implementation is detailed along with the D5.2.

### **4.3. Inspection Data Management**

The ground support system and its subsystems are shown in Figure 38. The inspection data from UT sensor equipment go to the UT ground subsystem and finally to the GSDB database and the operator user interface (UI).

The UT sensor equipment communicates through Ethernet cable to the aerial platform, where data are exchanged with the ground via a wireless link, reaching on the ground station, the UT ground subsystem, the GSDB and inspection engineer UI subsystem, and the pilot terminal, all connected by Ethernet cables through a switch.

The details of the above subsystems are given in D5.2.

## 5. Conclusions

This document has presented the final version of the HYFLIERS hybrid robot, the HMR and the HRA. The robots are based on the initial system specifications in the D1.1, the system concept architecture in D1.2 and the previous designs and robot concepts presented along with the D2.1 and D2.2.

The deliverable includes the detailed description of both HMR and HRA “as-built” and all their subsystems. At this stage of the project, the results collected in this deliverable (D5.1) in combination with the D5.2 and D5.3, show that both robot and their different subsystems were successfully tested through several experiments in controlled scenarios, and they are ready to start the validation phase along with the WP6. As conclusions, although there is a lot of pending work to reach industrial levels of TRLs, both systems seem to be promising solutions for their respective use cases.

Future deliverables (D5.3, D6.1 and D6.2) will specifically analyse the performance of both robotic systems during the preliminary testing of the integrated systems.



## References

- [1] M. A. Montes-Grova, F. J. Pérez-Grau and A. Viguria. “Multi-Sensor System for Pipe Inspection using an Autonomous Hybrid Aerial Robot”. Accepted for publication in *International Conference on Unmanned Aircraft Systems*, June 2022, Dubrovnik, Croatia.